Effects of Anisotropy and Multi-Axial Loading on the Wrinkling of Sandwich Panels

Linus Fagerberg and Dan Zenkert
KTH Aeronautical and Vehicle Engineering
SE-100 44, Stockholm, Sweden
E-mail: linus@kth.se, danz@kth.se

Abstract: Previously published work on sandwich face wrinkling almost always considers isotropic or almost isotropic sandwich configurations. In that case the critical wrinkling load only needs to be evaluated in the principal compressive stress direction. For a sandwich panel with a higher degree of anisotropy this is not enough. This paper presents a method for estimating the wrinkling behaviour of highly anisotropic sandwich panels under multi-axial loading. The method is based on the assumption that wrinkling occurs at the angle where the ratio of applied load to sustainable wrinkling loads reaches a global maximum. In addition to the description of the analytical theories the paper also contains comparisons with finite element calculations and testing of real sandwich configurations. The results indicate that the derived model works excellent both for uni- and bi-axial loading, though a small factor of safety is required as with all other standard wrinkling theories.

Keywords: wrinkling, local buckling, anisotropy, stability, sandwich

Introduction

Most theories on sandwich face wrinkling were derived using the assumption of isotropic sandwich constituents like most cellular foam cores and metal or quasi-isotropic fibre-reinforced plastic faces. These models always assumed that the wrinkling occurs perpendicular to the highest principal compression stress. For an anisotropic sandwich, this is not the case. The work presented in this paper was conducted in three different fields of practice, each providing parts to the whole theory and serving as a validation of the others; FE-analysis, analytical models and a test series. Parts of this paper have previously been published in [1]. In the present paper the theory is explained in more detail and is also validated with additional tests.

Basic wrinkling criteria

Hoff and Mautner [2], Plantema [3], Allen [4] and others have provided good analytical models for the 2D beam analogy of wrinkling. Using for example energy methods and the same assumption of exponential decay, as Plantema did, we end up with the following formula

$$P_{cr} = \frac{3}{2}\sqrt[3]{2D_f E_c G_c} \Rightarrow \sigma_{f,cr} = 0.85\sqrt[3]{E_f E_c G_c} \quad \text{for } v_f = 0.3 \tag{1}$$

As seen, this is very close to the result obtained by Hoff for the symmetrical case and thick core.

$$\sigma_{f,cr} = 0.91\sqrt[3]{E_f E_c G_c} \tag{2}$$

The only difference between Plantemas and Hoffs derivations is that different decay functions were used, otherwise the assumptions are the same. After some comparisons with tests, Hoff recommended that Equation (2) should be used with a knockdown factor and proposed that 0.5 should replace 0.91, in order to achieve a safe design. In the rest of this paper Equation (1) will be used as the wrinkling criteria.

Allen solved the wrinkling problem using a different method solving the differential equation for a beam (face) on an elastic substrate through the use of a stress function. His result was similar to the ones from Hoff and Plantema with the constant in front of the cubic root equal to 0.85 (for the poisson ratio of the core equal to 0.3).

These 2D design formulas for the uni-axial wrinkling case has previously been modified for use on panels subjected to multi-axial load. One approach where beam theory been extended to plate, has previously been verified by tests. Sullins et al. [5] only considered the principal axis of the plate and they suggested the following interaction formula as a wrinkling criterion

$$\frac{\sigma_1}{\sigma_{1cr}} + \left(\frac{\sigma_2}{\sigma_{2cr}}\right)^3 \leq 1 \quad \text{with } \sigma_1 > \sigma_2 \tag{3}$$

where the critical stresses σ_{1cr} and σ_{2cr} are the one-dimensional wrinkling stresses calculated in the directions of the principal stresses.

Vonach and Rammerstorfer [6] have also addressed the problem of wrinkling of orthotropic sandwich plates under general loading. They tackle the problem by assuming the core to be infinitely thick and the wrinkling wave at the interface between the face sheet and core to be sinusoidal. Thereafter they are able to solve the governing differential equation describing the face sheets deformation. Their approach gives almost the same result as the proposed solution described below but includes a complicated numerical minimisation procedure.

Wrinkling is still addressed by several researchers throughout the world. For example Niu and Talreja [7] have developed a unified wrinkling model combining the classical three modes of wrinkling and also shown that the anti-symmetrical mode is the critical one. Hadi and Matthews [8] has presented a development of the Benson-Mayers theory on the wrinkling of sandwich panels able to simultaneously calculate the anti-symmetric and symmetric wrinkling loads. Dawe and Yuan [9] has developed a B-spline finite strip method for predicting the buckling stresses of rectangular sandwich plates under the action of direct and shear stresses applied to the face sheets.

Strip theory model

The approach suggested in this paper is to calculate the wrinkling load by theoretically dividing the panel into thin strips, one in every direction. For each strip, the critical wrinkling load according to the usual 2D criterion is calculated and compared to the applied load. Wrinkling is assumed to occur in the direction of the strip, which has the highest ratio of applied load, compared to sustainable load. Cylindrical bending of the face sheet is assumed. The applied load may be found in any co-ordinate system by simple transformation of the applied loads N_x, N_y, and N_{xy}. P_φ is then simply taken as the compressive load in the studied direction φ, which

acts on one of the face sheets, see Figure 1a. Laminate theory can be used to calculate $P_{\varphi,cr}$ as a function of φ.

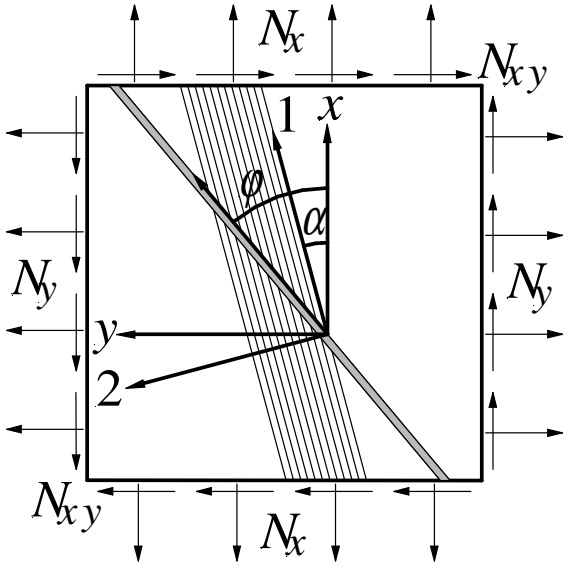

Figure 1a. An anisotropic sandwich plate subjected to multi-axial loading. The grey line symbolises the thin strip at the angle φ where the buckling load is evaluated.

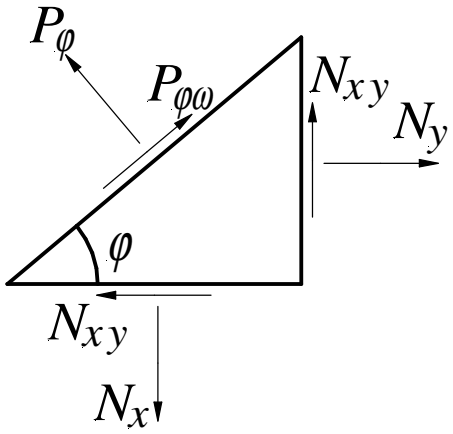

Figure 1b. Load definition.

For simplicity, assume a sandwich with an isotropic core and a face of one layer of an orthotropic fibre composite. The properties of the face can be expressed using the usual composite notation, e.g. Zenkert [10], with the stiffness matrix $\boldsymbol{Q}_{local}$.

$$\boldsymbol{Q}_{local} = \frac{1}{1-\nu_{12}\nu_{21}} \begin{bmatrix} E_1 & \nu_{21}E_1 & 0 \\ \nu_{12}E_2 & E_2 & 0 \\ 0 & 0 & G_{12}(1-\nu_{12}\nu_{21}) \end{bmatrix} \tag{4}$$

This local stiffness matrix is transformed to the global co-ordinate system using the transformation matrix $\boldsymbol{T}$.

$$T_\alpha = \begin{bmatrix} c^2 & s^2 & -2sc \\ s^2 & c^2 & 2sc \\ sc & -sc & c^2-s^2 \end{bmatrix} \text{ where } c=\cos(\alpha) \text{ and } s=\sin(\alpha). \tag{5}$$

Where α is the lay-up angle between the lamina and the global co-ordinate system, see Figure 1a. The global face stiffness matrix is then

$$Q_{global} = T_\alpha Q_{local} T_\alpha^t \tag{6}$$

The first position in this matrix $\boldsymbol{Q}_{global11}$, describes the stiffness in the global x-direction. To finally compute the face stiffness in an arbitrary direction, the φ direction, another transformation is required reading

$$Q_\varphi = T_\varphi Q_{global} T_\varphi^t \tag{7}$$

The first value in this matrix, $\boldsymbol{Q}_{\varphi 11}$, then describes the stiffness of the lamina in the φ direction. Inserting this into Equation (1) gives the critical stress $\sigma_{\varphi,cr}$

$$\sigma_{\varphi,cr} = 0.85\sqrt[3]{Q_{\varphi 11} E_c G_c} \tag{8}$$

Thus, we do not consider a new failure criterion in this model, only the way the criterion is evaluated. This method provides a possibility to calculate the angle between the applied load (or whichever reference of choice) and the wrinkling wave. The method is based on the assumption that the wrinkling first occurs at the angle φ where the ratio of applied load P_φ and sustainable wrinkling load $P_{\varphi,cr}$ reaches a global maximum.

If we let the face sheet be multi layered, comprising of several orthotropic laminae, the average Young's modulus of the face sheet no longer scales with the flexural rigidity (D_f) of the face sheet properly. The method to calculate the stiffness matrix of a composite plate is in detail described in [10] but can in short be explained with the following formula.

$$[\boldsymbol{A}, \boldsymbol{B}, \boldsymbol{D}] = \sum_{i=1}^{n} \boldsymbol{Q}_i \left[\left(z_i - z_{i-1}\right), \frac{1}{2}\left(z_i^2 - z_{i-1}^2\right), \frac{1}{3}\left(z_i^3 - z_{i-1}^3\right) \right] \tag{9}$$

By assuming the face sheet to have a symmetric lay-up sequence, or by simply neglecting the influence of the extension-bending coupling matrix, $\boldsymbol{B}$. $P_{\varphi,cr}$ is easily estimated by inserting the first value of the bending stiffness matrix, $\boldsymbol{D}_{\varphi 11}$, into Equation (1).

$$P_{\varphi,cr} = \frac{3}{2}\sqrt[3]{2 D_{\varphi 11} E_c G_c} \tag{10}$$

The core properties should of course also be transformed in the same manner as the face properties if the core is orthotropic in the plane.

Load transformation

Load equilibrium gives that the load and stress in the φ-direction can be calculated with the following simple transformation (see Figure 1b).

$$\begin{aligned} P_\varphi &= N_x c^2 + N_y s^2 - N_{xy} 2sc \\ \sigma_\varphi &= \sigma_x c^2 + \sigma_y s^2 - \tau_{xy} 2sc \end{aligned} \tag{11}$$

Wrinkling hypothesis

The hypothesis forming the wrinkling criterion is that wrinkling occurs when the applied load in any direction P_φ (Equation (11)) equals the critical uni-axial wrinkling load $P_{\varphi,cr}$ (Equation (10)). Thus, by multiplying the applied load by an arbitrary load factor λ, we get that wrinkling occurs when

$$\lambda P_\varphi \geq P_{cr,\varphi} \text{ for any angle } \varphi \tag{12}$$

The load factor λ is thus given the minimum value

$$\lambda = \min_\varphi \frac{P_{cr,\varphi}}{P_\varphi} \tag{13}$$

Calculated example

Using the presented analytical approach on the test material configuration, see Table 1 and 2, gives the following results for a specimen with a 15° angle (α) between the fibre and load. The applied initial load was set to N_x = 50 kN/m and $N_y = N_{xy} = 0$.

Material Property	Value
E_1	107 GPa
E_2	15 GPa
G_{12}	4.3 GPa
ν_{12}	0.3
t	0.5 mm

Table 1. Measured face sheet material properties.

Material Property	Value
E_c	20 MPa
G_c	10 MPa
ν_c	0.25

Table 2. Material properties for Divinycell H30.

Material Property	Value
E_c	56 MPa
G_c	22 MPa
ν_c	0.25

Table 3. Material properties for Divinycell H60.

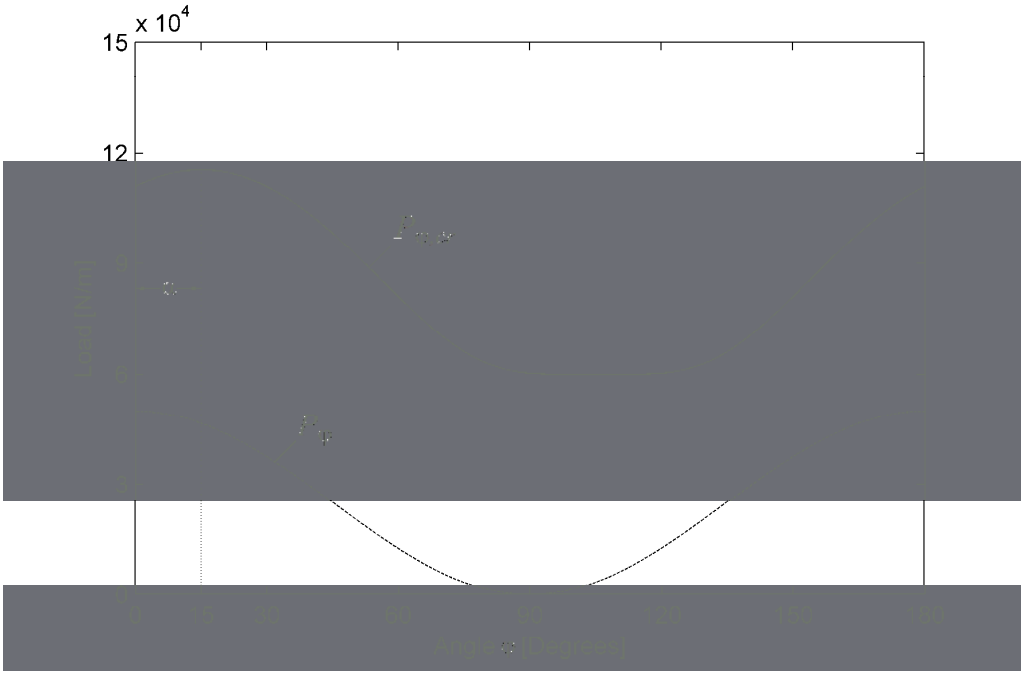

Figure 2. Results from the analytical approach calculations on a sandwich plate with fibre angle $\alpha = 15°$. The diagram shows $P_{\varphi,cr}$, P_{φ}. versus φ for the calculated example. An illustration of α is also included in the figure.

Figure 2 shows the variation of $P_{\varphi,cr}$ and P_{φ}. The form of P_{φ} is sinusoidal, which stems from Equation (11), while $P_{\varphi,cr}$ exhibits a quite different shape. Since P_{φ} in the calculated example is zero for $\varphi = 90°$, λ tends to infinity close to that angle. Therefore it is convenient to instead plot $1/\lambda$ as shown in Figure 3.

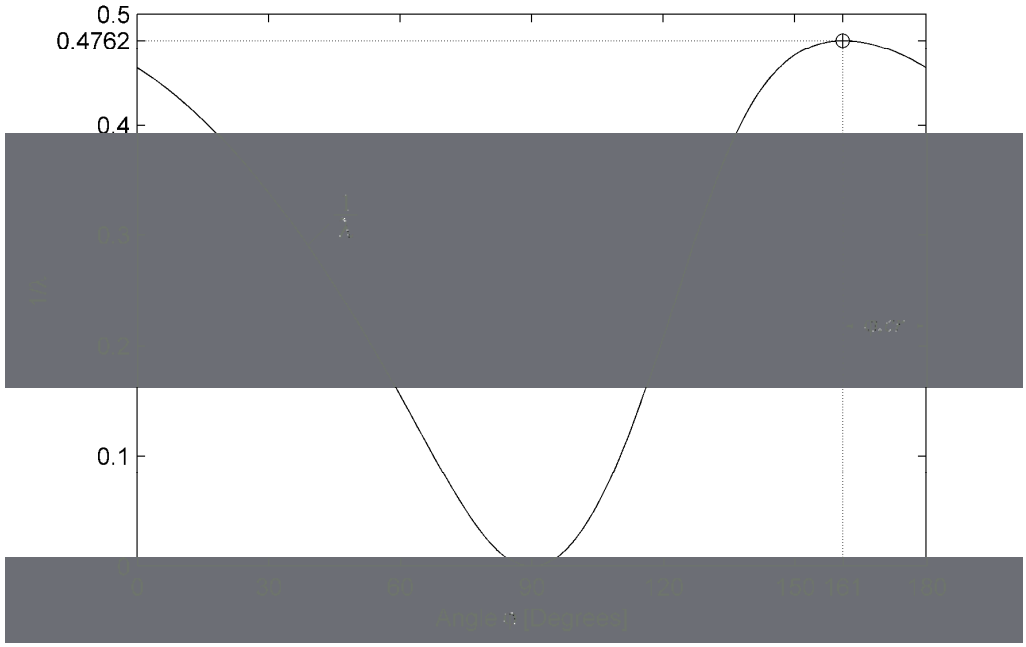

Figure 3. Results from the analytical approach calculations on a sandwich plate with fibre angle $\alpha = 15°$. The figure shows $1/\lambda$ versus φ for the calculated example. Included in the figure is also an illustration of φ,cr.

It can be seen that 1/λ has its maximum for $\varphi = -19°$, i.e. the wrinkling will occur at a skew angle of $\varphi = -19°$. Figure 3 also shows that the maximum of 1/λ is equal to 0.4762, or $\lambda = 2.100$. Then, the applied at onset of wrinkling is given by

$$MaxAppliedLoad = \lambda \cdot InitialAppliedLoad = 2.100 \cdot 50kN/m = 105kN/m \quad (14)$$

This can be seen as multiplying the curve for P_φ until it at some point (at some angle φ) reaches the curve for $P_{\varphi,cr}$, as illustrated in Figure 4. The point of interception gives the off wrinkling angle φ,cr and the scale factor is simply the load factor λ.

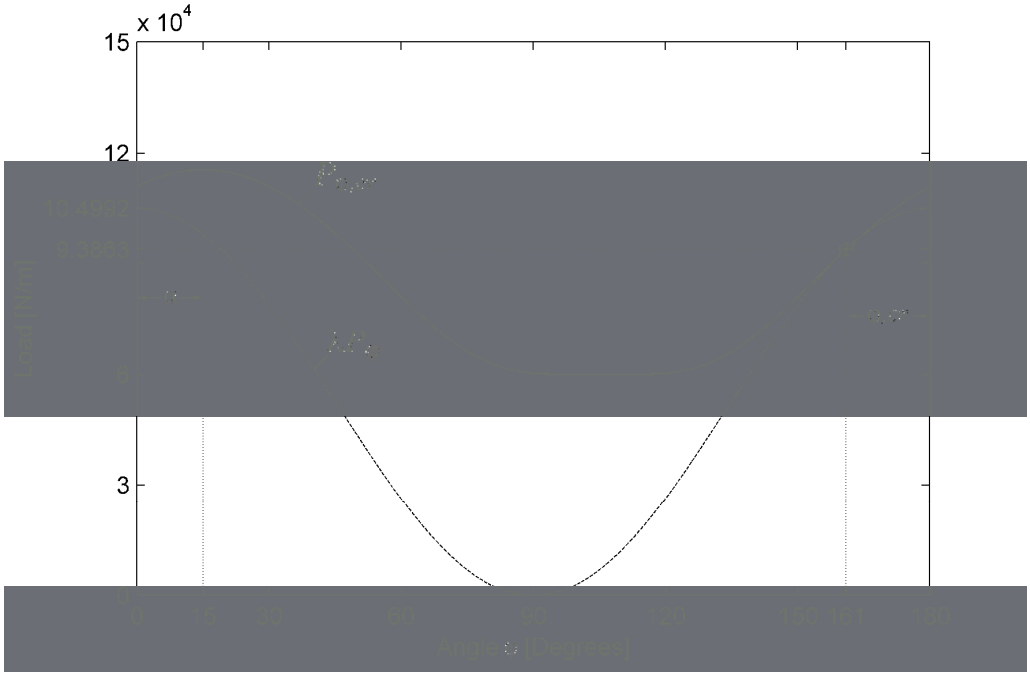

Figure 4. Results from the analytical approach calculations on a sandwich plate with fibre angle $\alpha = 15°$. $P_{\varphi,cr}$ and λP_{φ} versus φ for the calculated example. Included in the figure is also $\varphi_{,cr}$ and α illustrated.

Experimental validation and FE-calculations

A test series was used to investigate the phenomenon of wrinkling in anisotropic sandwich panels. In the first test series 14 panels where tested under uni-axial loading with different angle between the load and the principal axis of the sandwich plate. In the second study a series of 18 panels were tested under bi-axial loading. In this test series the investigation focused on different ratio between the load in each direction and only a few different angles between the load and the principal axis of the plate were studied. Both test series where compared with finite element calculations and with the analytical approach described in this paper. The test specimens were small sandwich plates, 200 by 150 mm, with 25 mm wide tabs fitted to each loaded edge, see Figure 5a. The loaded edges where very carefully milled until they where parallel.

Uni-axial loading

The sandwich material configuration, which was used in the tests, was a 50 mm thick Divinycell H30 core with faces of two layers of uni-directional T700 carbon fibres in a vinylester matrix. The core was selected extremely weak insuring wrinkling as the predominant failure mode. Strips of the face material were also used to measure the material properties, which are given in Table 1. The core material properties given in Table 2 is a lower bound taken from the technical specification provided by the manufacturer.

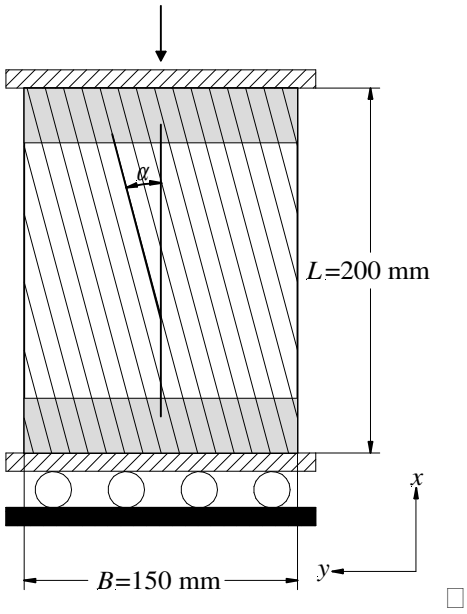

Figure 5a. Schematic of test set-up showing specimen dimensions and fibre angle.

Figure 5b. Tested specimen after failure still subjected to load.

Test set-up

The set-up used an Instron test machine and a pair of steel plates with roller bearings, see Figure 5a. The bearings were necessary in order to allow global in-plane shear deformations that will occur at fibre angles different from 0º and 90º even under uni-axial loading.

Figure 5b is a photograph of a test specimen just after wrinkling has occurred and the skew wrinkling is clearly visible. This specimen failed inward in face sheet wrinkling failure on one side and outward on the other side. It is likely that the outward buckling of the reverse side is a secondary failure, which appeared on some test specimens. This face sheet was, however, still intact although separated from the core.

Finite element analysis

Linear elastic finite element (FE) calculations on the wrinkling stability problem were performed with the FE-code ABAQUS. The model simulated the tested specimen and was modelled using 20-node brick elements for the core and 8-node shell elements for the composite face sheets. A plot of the mesh is shown in Figure 6. All materials were considered linear elastic and the material properties used are given in Tables 1 and 2. The edge load was distributed using multi-point constraints. The loaded edges of the panel (horizontal in Figure 5a) were modelled flat and parallel to each other. The model allowed shear in the plane (x-y plane) of the face sheets but no twisting of the loaded edges were allowed. The loaded edges of the face sheet where locked in rotation around the axis of the edge (y-axis) to prevent localized buckling at the load introductions. The tabs of the real specimens provide a similar boundary condition. The buckling load was calculated using eigenvalue buckling procedures within the FE program.

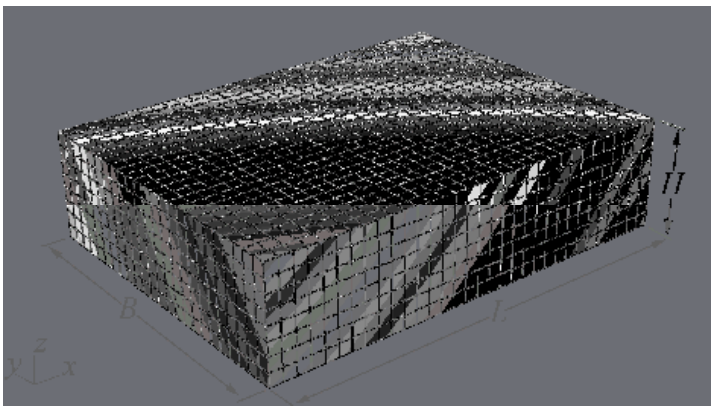

Figure 6. Finite element model. Mesh, coordinate system and dimensions.

The mesh density of the FE model is fine enough to provide a good estimate of the buckling load but a bit too coarse to smoothly model the actual shape of the wrinkling mode. Based on experience two elements per half wrinkling wavelength is enough to capture the buckling load with reasonable accuracy but to model the mode shape smoothly at least four elements is recommended. The core also has to have at least four elements though the thickness, otherwise the model acts too stiff and predicts a higher buckling load than if enough elements is used. The choice of mesh density for the model is further based on the computer power available. It took approximately 50 minutes to solve the first two eigenvalues of the described model on Linux workstation.

Results

A total of 14 specimens with different fibre angles were successfully tested. Specimen 9 and 10 failed in wrinkling out from the core not leaving any means to determine the wrinkling angle. Specimen 4 and 5 failed at a considerably lower load than predicted, probably as a result of imperfect specimen preparation. All results from tests, FE analysis and the proposed analytical approach are presented in Figure 7a and 7b.

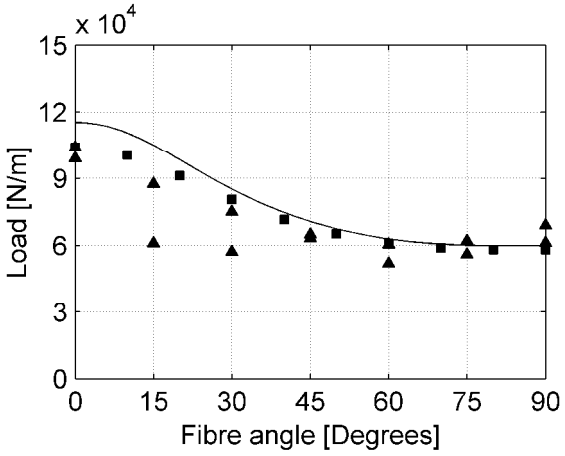

Figure 7a. Wrinkling load (P_{cr}) versus fibre angle α. Black line is illustrating the results from the strip theory. Squares show FE calculations. Triangles show test results.

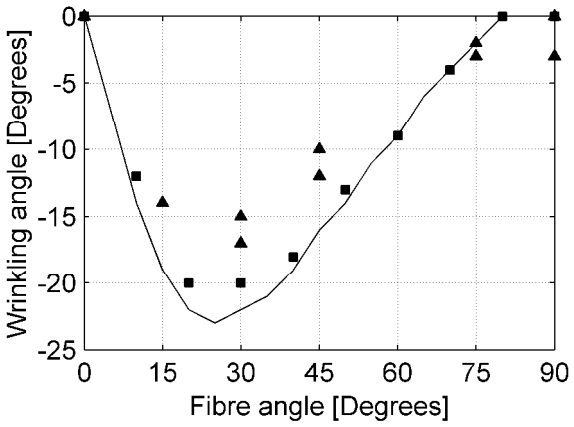

Figure 7b. Wrinkling angle (φ_{cr}) versus fibre angle α. Black line is illustrating the results from the strip theory. Squares show FE calculations. Triangles show test results.

The analytical calculations, black solid line in Figure 7a, were calculated with the analytical approach given in Equation (10). If one had used the knockdown factor as Hoff has recommended the line would be below the test results (triangles in Figure 7a) instead of above. The FE calculations (squares in Figure 7a) are in good agreement with both tests and analytical solution. The slight overestimation in wrinkling load for small α may probably partly be due to a too high estimated Young's modulus in the fibre direction of the face sheet. This was based on traditional tension testing of strips of the face sheet material and the compressive modulus is often somewhat lower than the tensile modulus.

The results concerning wrinkling angle also shows good agreement between the numerical methods and test results, see Figure 7b. The reason why the analytical curve is not entirely smooth is that the load factor was only evaluated for every whole degree. This gives a small discontinuity in the results. The trends are however clearly visible and agree well through all calculations and tests. It is apparent that the FE model and tests are more conservative regarding the wrinkling angle than the analytical model. This is however expected since both suffer from edge effects where the boundaries of the plate enhance a buckling pattern that strives to be parallel to the edges. Since the analytical model does not include this effect it predicts more extreme wrinkling angles. The proposed approach still shows remarkably good agreement with the results from FEM and tests, both concerning predicted wrinkling load and angle φ_{cr}.

Bi-axial loading

In the second test series, consisting of 18 panels, the focus was on the effect of multi-axial loading. The test specimens were similar to the ones from the first series regarding dimensions and face material. The core material came from the same manufacturer but was of the H60 grade, see Table 3 for material properties supplied by manufacturer. These are the lower bounds from the technical specifications. For the calculations the initial load vector $[N_x\ N_y\ N_{xy}]$ was set to $[1, r, 0]$.

$$r = \frac{N_y}{N_x},\ 0 \le r \le 1 \tag{14}$$

Test set-up

To apply the bi-axial loading a test rig was manufactured. This test rig was kept as simple as possible and consisted of two steel plates, two sheaves and a pair of wires with pre-pressed threaded end fittings. A special pair of load cells where also manufactured using a pair of steel tubes and strain-gauges. These load cells where calibrated in the same Instron test machine as the actual test was performed and was re-calibrated between every third test to minimize measurements errors. The reason why wires where used instead of steel rods or anything similar was that with the wires and sheaves it was sufficient with only two extra load cells instead of four. The wires also allowed shearing of the specimen more freely than rods would have.

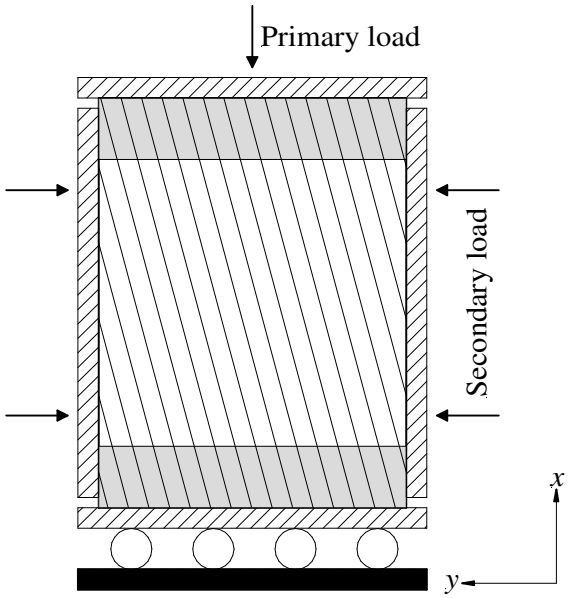

Figure 8a. Schematic of test set-up for the bi-axial loading test series.

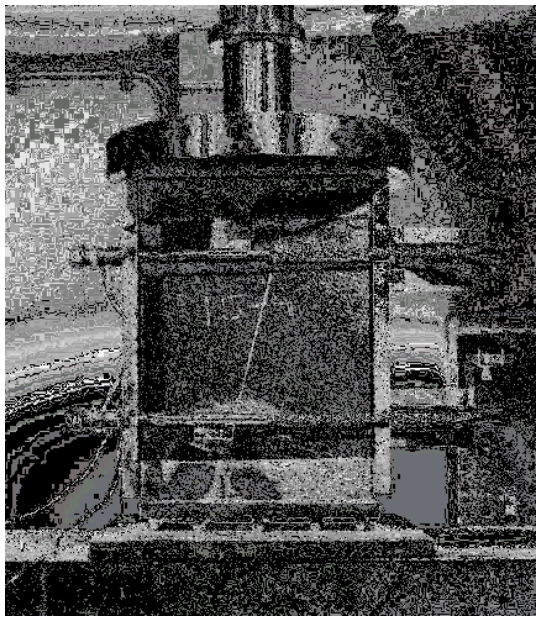

Figure 8b. Test setup for the bi-axial test series showing one of the test specimens mounted in the test machine.

Before the specimen was inserted in the testing machine the transverse load was applied using a regular spanner while the readings from the load cells were monitored. After a suitable amount of transverse load (P_y) been applied, the specimen was mounted in the testing machine. The specimen was thereafter subjected to a compressive load and both the readings from the extra load cells and the load cell of the machine here simultaneously monitored until the specimen failed. After the test had been completed these readings were used to decide both ultimate compressive force (P_x) and the value of r.

Finite element analysis

The finite element model used for the bi-axial loading case was very similar to the model already described. In fact exactly the same model was used (with altered material properties) in the cases where $r = 0$. In addition to the uni-axially loaded model the bi-axially loaded one includes more multi-point constraints. The additional constraints are forcing the edges where the secondary load is applied (vertical in Figure 8a) to remain flat. This is similar to the loading conditions in the tests, see steel plates in Figure 8a and 8b.The secondary loaded face sheet edges is also locked in rotation around their own axis (x-axis). The secondary loaded areas are not forced to remain parallel to each other or perpendicular to the primary loaded edges and hence still allow the panel to shear (in the x-y plane).

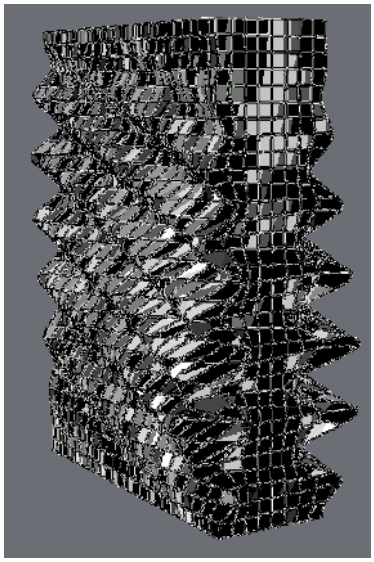

Figure 9a. Finite element model showing the first buckling mode of a uni-axially loaded sandwich panel with α = 30°.

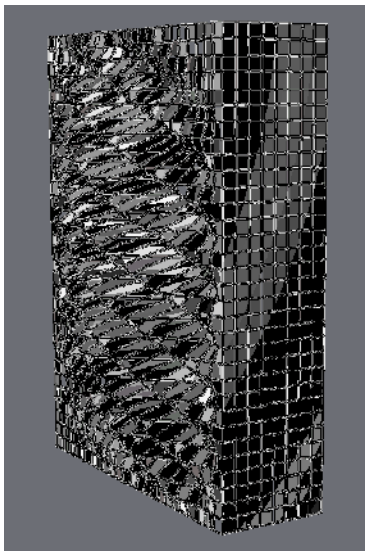

Figure 9b. FE model showing the first buckling mode of a bi-axially loaded sandwich panel with α = 30° and r = 0.4.

This FE model closely simulates the test set-up, but still quite far from the assumptions made in the analytical approach. For example, the wrinkling pattern is not describing pure cylindrical bending of the face sheets and cannot be described with a simple sinusoidal wave pattern. The buckling waves is two-dimensional with one half wave across the width of the plate and several waves in the length direction, see Figure 9b. Hence the buckling pattern is not truly periodic and it might be discussed if it is truly wrinkling (in the meaning of periodic buckling with a natural wavelength) or not. The boundary effects of the plate become more important and these increase the predicted buckling load and decrease the wrinkling angle compared to the analytical model. This effect was not as pronounced in the uni-directionally loaded panels, see Figure 9a. It is possible to use a FE model with periodic boundary conditions, see [1] and [6]. Such a model is closer to the analytical assumptions but more far from the test-setup.

Test results

All test results together with the predictions from FE calculations and the analytical model are given in Figs.10-12. In all figures the predictions from the analytical model are given by a full line. The values from the FE simulations are marked with squares and finally the test values are shown with triangles.

Figure 10a and 10b show the results for the panels with $\alpha = 0°$, i.e., with the fibres oriented in the x-direction. The FE calculations and analytical model are in very good agreement for r values lower than 0.4. At higher r values the FE calculations predict a higher load than the analytical model. Regarding the wrinkling angle, shown in Figure 10b, the FE model failed to predict the wrinkling angle for high r values (high transverse load) since the predicted eigenvalue mode consisted of superimposed wrinkling patterns with φ equal to 0° and 90°. For very high r values the FE calculations predicted localized buckling at the corners of the steel plates distributing the secondary load. The test results show the same trends as the analytical and FE models but with a somewhat lower wrinkling load. The wrinkling angles obtained from

the tests are in good agreement with the predicted values. It was not possible to investigate higher r values than 0.3 in the experiments.

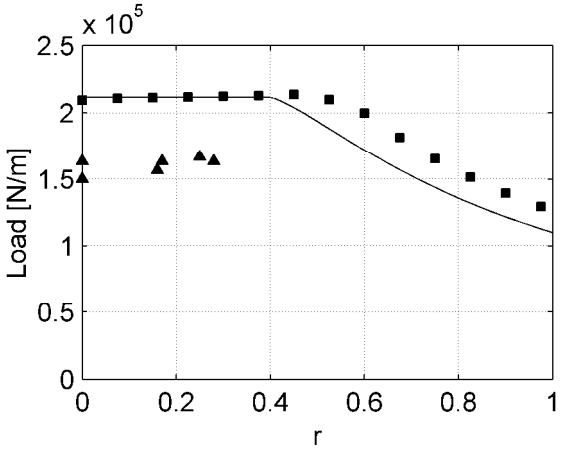

Figure 10a. Wrinkling load versus r for a sandwich plate with $\alpha = 0°$. Black line is illustrating the results from the strip theory. Squares show FE calculations. Triangles show test results.

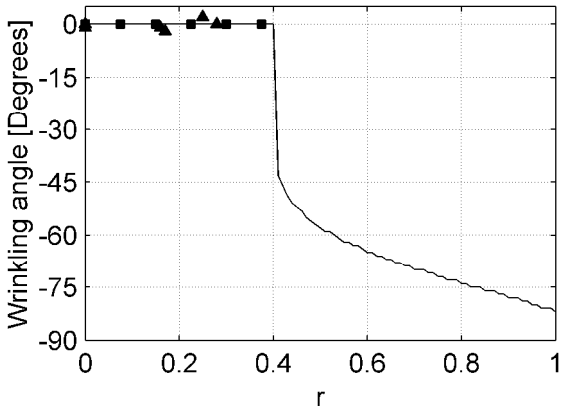

Figure 10b. Wrinkling angle versus r for a sandwich plate with $\alpha = 0°$. Black line is illustrating the results from the strip theory. Squares show FE calculations. Triangles show test results.

Figure 11a and 11b show the results for the panels with $\alpha = 15°$. The trends are similar to the ones described earlier. The FE predictions for the load are higher than the analytical predictions while the angles are more conservative in the FE model. The failure loads from the tests where a bit lower than predicted. Noticeable is that the tested panels with r close to 0.2 gave higher loads than the ones from uni-directionally loaded panels ($r = 0$). This is probably due to the previously described change in buckling mode shape when applying the transverse load. The FE calculations could be used to predict wrinkling angles for $r < 0.7$. The highest r value in this series was almost 0.5.

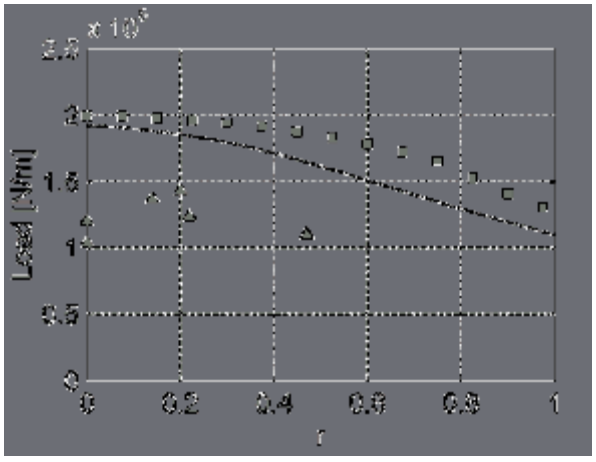

Figure 11a. Wrinkling load versus r for a sandwich plate with $\alpha = 15°$. Black line is illustrating the results from the strip theory. Squares show FE calculations. Triangles show test results.

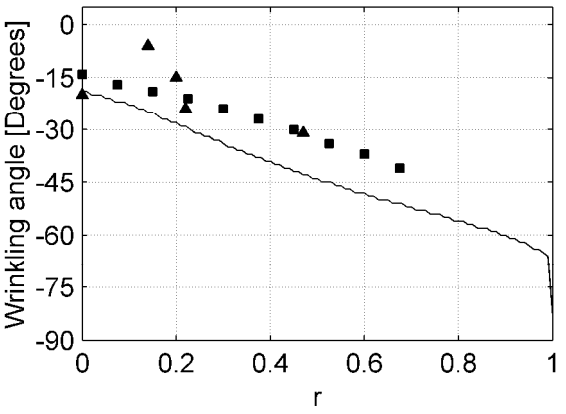

Figure 11b. Wrinkling angle versus r for a sandwich plate with $\alpha = 15°$. Black line is illustrating the results from the strip theory. Squares show FE calculations. Triangles show test results.

Figure 12a and 12b show the results for the panels with $\alpha = 30°$. Exactly the same trends as previously described can be seen. The FE calculations give highest buckling load and tests the

lowest. For the wrinkling angle, the FE calculations are more conservative than the analytical model. Noticeable also that for this fibre angle is that the low *r*-value specimens gave a somewhat higher load than the uni-directionally loaded ones. The FE calculations could be used to predict wrinkling angles for $r < 0.8$. The highest *r* value in this series was 0.6.

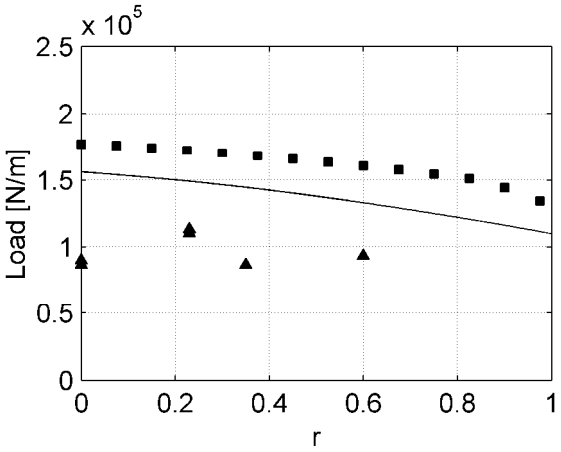

Figure 12a. Wrinkling load versus *r* for a sandwich plate with $\alpha = 30°$. Black line is illustrating the results from the strip theory. Squares show FE calculations. Triangles show test results.

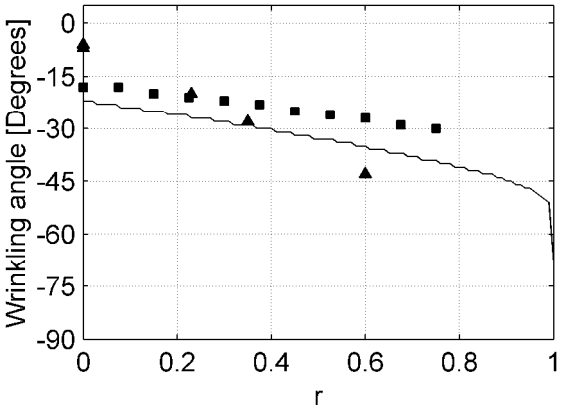

Figure 12b. Wrinkling angle versus *r* for a sandwich plate with $\alpha = 30°$. Black line is illustrating the results from the strip theory. Squares show FE calculations. Triangles show test results.

Relevance

It is obvious that the effect of skew wrinkling can be significant. How large the effect is depends on the degree of anisotropy of the face sheets and how the panel is loaded. Figure 13 shows the difference between the critical wrinkling stress calculated with and without respect to off angle wrinkling for a sandwich with the previously presented material properties (Table 1 and 2).

The calculations presented in Figure 13 shows that the traditional approach where skew wrinkling is not included in the analysis overestimates the wrinkling load by as much as 16%. The traditional approach assumes that wrinkling occurs perpendicular to the maximum compressive stress. This overestimation is generic and does not only appear in purely uni-directional laminates. As soon as the bending stiffness in the face sheet is significantly higher in one direction than in others and the loads are not aligned with the principal directions of the laminate skew wrinkling will occur.

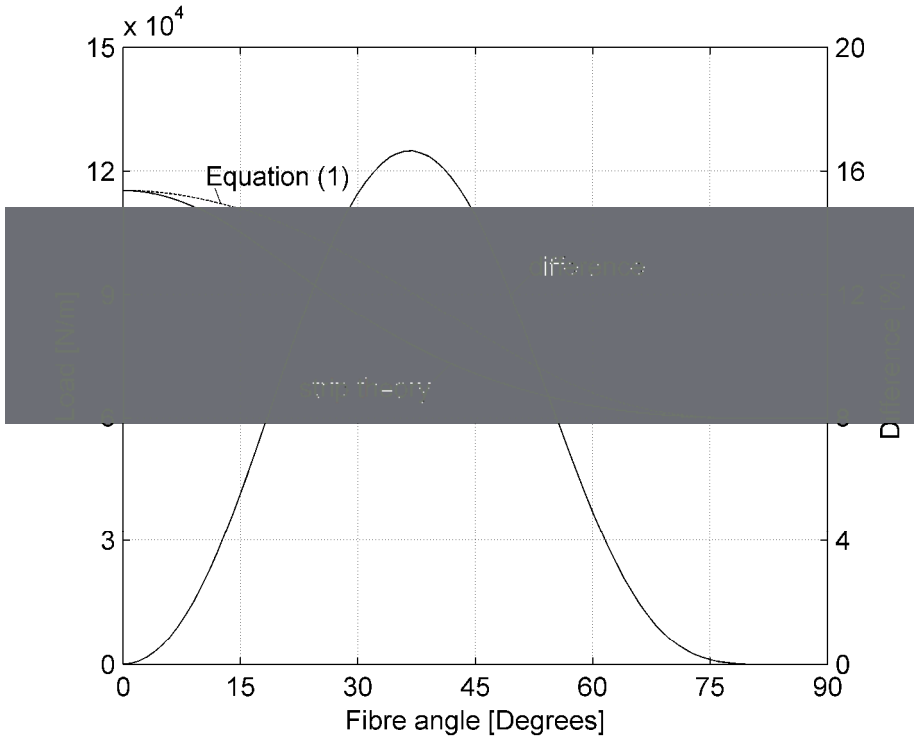

Figure 13. Wrinkling load versus fibre angle α, calculated with and without consideration of skew wrinkling. The difference is also expressed in percent and plotted versus the right y-axis.

Conclusions

The presented method is easy to use and gives according to this evaluation good prediction of the critical wrinkling load. The actual analytical model can be considered conservative since it predicts the minimum wrinkling load and includes the effects of skew wrinkling. But since the actual wrinkling condition in itself is not changed it is still recommended to use a knock down factor, as Hoff and others have suggested, to design safely.

The testing validates that the model can be used for uni-axial loading of anisotropic sandwich panels, and also for bi-axial loading, at least while one load component is less than approximately 30% of the major one. It should be noted, however, that test set-up does not exactly comply with the analytical model, due to boundary effects. The FE-calculations are, one the other hand, a more realistic model of the tests. In reality, the boundary effects are surely different, the sandwich panels commonly larger and the free-field assumptions used in the analytical model could be more adequate.

It would be interesting to see even more validation testing done on this approach using more sophisticated testing equipment. More testing could also be performed on sandwich plates with a more complex face sheet lay-ups instead of the uni-directional, which was used in this study. The approach seems to have a large potential and it is a good compliment to tests and faster to use then FE-analyses.

Acknowledgements

This work was funded by The Swedish Defence Materiel Administration, FMV Contract 63823-LB109101, and was conducted with support from Kockums AB Karlskronavarvet.

References

[1] Fagerberg L., "Wrinkling of Anisotropic Sandwich Panels Subjected to Multi-Axial Loading", *Sandwich Construction 5 – Proceedings of the 5th International Conference on Sandwich Construction*, Ed. H.-R. Meyer-Piening and D. Zenkert, EMAS Publishers, London, pp. 211-220, 2000.

[2] Hoff N.J. and Mautner S.E., "Buckling of Sandwich Type Panels", *Journal of the Aeronautical Sciences*, Vol. 12, No 3, pp. 285-297, 1945.

[3] Plantema F.J., *Sandwich Construction*, John Wiley & Sons, New York, 1966.

[4] Allen H.G., *Analysis and Design of Structural Sandwich Panels*, Pergamon Press, Oxford, 1969.

[5] Sullins R.T., Smith G.W. and Spier E.E., "Manual for Structural Stability Analysis of Sandwich Plates and Shells"!, *NASA-Contractor Report No. 1467*, 1969.

[6] Vonach W.K., Rammerstorfer F.G., "Wrinkling of thick orthotropic sandwich plates under general loading conditions", *Archive of Applied Mechanics*, Vol. 70, pp. 338-348, 2000.

[7] Niu K. and Talreja R., "Modeling of Wrinkling in Sandwich Panels Under Compression", *Journal of Engineering Mechanics*, Vol. 125, pp. 875-883, 1999.

[8] Hadi B.K., "Development of Benson-Mayers theory on the wrinkling of anisotropic sandwich panels", *Composite Structures*, Vol. 49, pp. 425-434, 2000.

[9] Dawe D.J. and Yuan W.X., "Overall and local buckling of sandwich plates with laminated faceplates, Part I: Analysis", *Computer methods in applied mechanics and engineering*, Vol. 190, pp. 5197-5213, 2001.

[10] Zenkert D., *An Introduction To Sandwich Construction*, EMAS Ltd, Warley, UK, 1995.